# Using CFD Technology to Simulate a Model of Human Thermoregulation in the Stable Temperature Environment

Sina Dang[1], Hongjun Xue[1(✉)], Xiaoyan Zhang[1,2,3], Jue Qu[1],
Chengwen Zhong[1], and Siyu Chen[1]

[1] School of Aeronautics, Northwestern Polytechnical University, Xi'an, China
dsnsw123@126.com, {xuehj,zhongcw}@nwpu.edu.cn,
qujue402@sina.com, zxyliuyan@163.com,
szll0000.csy@163.com
[2] Institute of Human Factors and Ergonomics, Shenzhen University,
Shenzhen, China
[3] Key Laboratory of Optoelectronic Devices and Systems
of Ministry of Education and Guangdong Province,
Shenzhen University, Shenzhen, China

**Abstract.** A coupling system was developed in the present study to simulate the heat transfer and physiological responses of the unclothed human body in hot and cold environments. This system included a computational thermal manikin controlled by a multi-node thermal model, which could dynamically respond to the environmental conditions. The computational thermal manikin was employed to determine the heat transfer between the human body and ambient environment as well as heat transfer coefficients at each body segment. The CFD simulation was then coupled with a multi-node thermal model to predict the heat transfer and human physiological responses in real time. The performance of coupling system was examined by comparing the simulated skin temperatures with the published measurements from human trials in hot and cold environments. The coupling system reasonably predicted the skin temperatures at local body segments with the maximum discrepancies between the observed values and simulated ones no more than 1.0 °C.

**Keywords:** Heat transfer · CFD simulation · Environment conditions · Response

## 1 Introduction

Over the past few decades, many computational thermal manikins ranging from a rectangle to multi-zone have been constructed to resemble the human body. CFD simulation [1] has become a useful tool to calculate heat flux between the human body and ambient environment and heat transfer coefficients using these computational thermal manikins in virtual environments [2]. However, the computational manikin did not contain a thermoregulation system and could not respond to the environment as human beings. Meanwhile, a large number of thermal models [3] have been developed to simulate human thermal responses under transient environments. It is therefore

necessary to combine the CFD program with the thermal models to better understand the heat transfer and thermal physiological responses [4].

In this study, the three-dimensional model was developed, based on the Fiala's [5] model. It can predict physiological response for stable temperature environments, with taking into consideration of the effects on the pulsatile laminar flow, the peripheral resistance, the thermal effect of food and the composition of viscera [6]. Using the CFD technology to simulate the whole-body 3D human thermoregulation model. This model makes use of the finite volume method to discretize the heat conduction of the differential equation concerning the human body, calculates the distribution of blood flow velocity, pressure and temperature by means of a one-dimensional N-S equation [7], and finally solves numerical values with the CFD method and obtains the change curve of the human body's temperatures with time.

## 2   CFD Simulation

### 2.1   Use CFD to Build the Body's Geometric Model and Vascular Geometry Model

A geometric model of human body is established in this paper. This paper select the basic size of human body with height of 174.9 cm, body weight of 66.3 kg and surface area of 1.86 m$^2$. The i (1–18) shows the human body. The human body is divided into the head, the front 1/2 and the back 1/2 of the head, the neck, the front 2/5 of the trunk, the middle 1/5 and the back 2/5, the upper arm, the lower arm, the hands and thighs, the calves and feet. A total of 18 segments. The k (1–5) is used to represent the layers of human body, which is divided into visceral layer, skeletal layer, muscular layer, fat layer, skin, j (1–7) to represent human visceral organs such as brain, lung, heart, liver, stomach, large intestine, small intestine etc. The specific geometric data of each layer is shown in Table 1 [8]. In order to reduce the difficulty of simulation, the viscera is simplified the regular graphics with CFD. The geometric size of the human body and the geometric size of the blood vessels are modeled through ANSYS 19.0.

Take 1, 2 as a whole, as the heart output. It's length 6 cm, radius 1.285 cm, thickness of blood vessel wall 0.147 cm. Take 3–9 as a whole, as the trunk aorta, length 35.4 cm, radius from 1 cm–0.57 cm uniform change of conical blood vessels, blood vessel wall also changes from 0.12 cm–0.08 cm. Take 10–13 as one, with a length of 32.9 cm, a radius of 0.57–0.24 cm, and a blood vessel wall of 0.08–0.05 cm. Take 14–19 as one, with a length of 65.8 cm, a radius of 0.24–0.13 cm, and a blood vessel wall of 0.05–0.019 cm. Take 20–29 as one, with length 63.5 cm, radius 0.4–0.19 cm, vascular wall 0.062–0.046 cm. 30–35 is the head artery, the length is 39.5 cm, the radius is 0.37–0.06 cm, and the blood vessel wall is 0.063–0.02 cm. The simplified geometric model is shown in the Fig. 1.

**Table 1.** Human modeling geometric data.

| i | Segment | L(cm) | Major semiaxis / Semi-minor axis | | | | | Sketch Map |
|---|---------|-------|------|------|--------|-----|------|------------|
| | | | core | bone | muscle | fat | skin | |
| 1 | Head | 11.05 | 17.92/ 16.59 | 18.62/ 17.06 | 22.62/ 21.06 | 23.02/ 21.46 | 23.4/ 21.84 | |
| 2 | face | 11.05 | - | 18.62/ 17.06 | 22.62/ 21.06 | 23.02/ 21.46 | 23.4/ 21.84 | |
| 3 | neck | 11.9 | - | 1.4/ 1.43 | 4.01/ 4.04 | 4.37/ 4.39 | 4.69/ 4.72 | |
| 4 | chest | 20.87 | 20.1/ 13.46 | 28.17/ 21.53 | 29.58/ 22.95 | 31.97/ 25.33 | 32.46/ 25.8 | |
| 5 | Abdomen | 10.43 | 28.17/ 21.53 | 10.5/ 4.035 | 29.58/ 22.95 | 31.97/ 25.33 | 32.46/ 25.8 | |
| 6 | Waist | 20.87 | 28.17/ 21.53 | 10.5/ 4.035 | 29.58/ 22.95 | 31.97/ 25.33 | 32.46/ 25.8 | |
| 7 | L- upper arm | 30.77 | - | 5.3/ 4.9 | 10.2/ 9.8 | 11.1/ 10.7 | 11.57/ 11.2 | |
| 8 | R- upper arm | 30.77 | - | 5.3/ 4.9 | 10.2/ 9.8 | 11.1/ 10.7 | 11.57/ 11.2 | |
| 9 | L- lower arm | 22.61 | - | 5.31/ 4.18 | 9.77/ 8.65 | 10.59/ 9.47 | 11.0/ 9.9 | |
| 10 | R- lower arm | 22.61 | - | 5.31/ 4.18 | 9.77/8.65 | 10.59/ 9.47 | 11.0/ 9.9 | |
| 11 | L-hand | 17 | - | 6.44/ 1.84 | 6.98/ 2.38 | 7.81/ 3.22 | 8.8/ 4.2 | |
| 12 | R-hand | 17 | - | 6.44/ 1.84 | 6.98/ 2.38 | 7.81/ 3.22 | 8.8/ 4.2 | |
| 13 | L-thigh | 42.67 | - | 6.74/ 7.14 | 14.95/ 15.36 | 16/ 16.4 | 16.63 /17 | |
| 14 | R-thigh | 42.67 | - | 6.74/ 7.14 | 14.95/ 15.36 | 16/ 16.4 | 16.63/ 17 | |
| 15 | L-leg | 35.57 | - | 6.75/ 6.91 | 12.56/ 12.72 | 13.47/ 13.63 | 13.96/ 14.1 | |
| 16 | R-leg | 35.57 | - | 6.75/ 6.91 | 12.56/ 12.72 | 13.47/ 13.63 | 13.96/ 14.1 | |
| 17 | L-foot | 23.8 | - | 1.81/ 1.2 | 2.69/ 2.09 | 4.14/ 3.54 | 5.37/ 4.77 | |
| 18 | R-foot | 23.8 | - | 1.81/ 1.2 | 2.69/ 2.09 | 4.14/ 3.54 | 5.37/ 4.77 | |
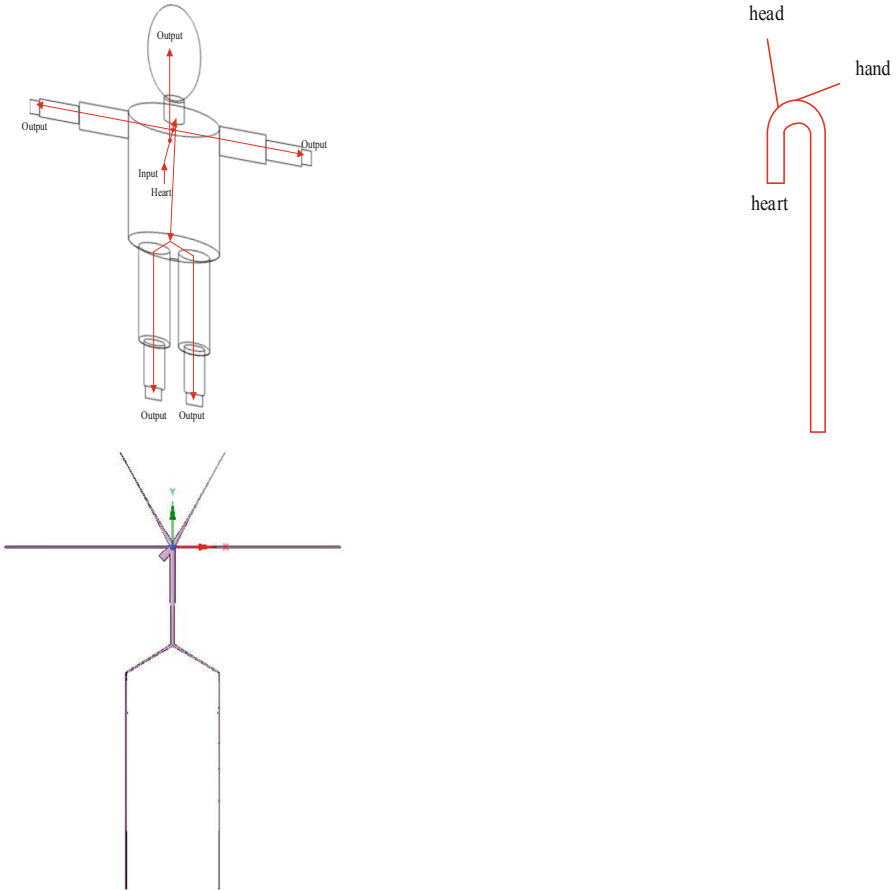
**Fig. 1.** The geometric size of the blood vessels.

## 2.2   Computational Grid

Grid division based on the established geometric model of human body and vascular model It was difficult to resolve the complex geometry of the numerical manikin by a structured grid [9]. The unstructured grids were used for the body and the blood models. The human geometric model and the grid division of blood vessels are shown in the figure. The human geometry model contains 2400580 cells and 8569224 nodes, and the vascular models contains 52368 cells and 50175 nodes.

The commercial CFD software ANSYS was used to simulate the heat transfer between the human body and environment. In addition to using ANSYS to solve the equations, the mathematical simulation of the human thermal regulation model also needs to use UDF to compile the equations proposed in this paper.

## 2.3    Coupling the CFD Simulation with the Thermal Model

Before calculating the change of human temperature over time, the initial human temperature must be given. The core temperature of the human body can be measured by a thermometer, and the skin temperature can also be measured by a skin temperature meter. But the internal initial temperature is uncertain. Therefore, the initial temperature value of each node of the human body in this paper is given as fellows. The body is first considered as a steady state, no internal heat source object, and the internal core layer boundary and skin surface temperature are calculated to obtain a specific initial temperature. The process of calculating the initial temperature using CFD is as Fig. 2.

After calculating the initial temperature, setting the time step, this paper takes the time step length to 0.1 s. The temperature of the outlet section of the heart is used as the output value of the blood vessel temperature. Given the pulsating pressure and velocity curve, the distribution of blood vessel temperature is solved by using the N-S equation. Exporting the vascular boundary temperature at each point of the blood vessels mentioned above, the perfusion temperature is calculated by using the formula, and the perfusion temperature is assigned to the heat source in the heat transfer of human tissues, so that the human heat transfer under unsteady state can be calculated.

The heat source items of human heat transfer include blood perfusion heat production and metabolic heat production. This makes the human body's heat transfer become a heat transfer problem that contains an internal heat source under unsteady state. Heat transfer problems with internal heat sources. On the surface of the human skin, heat exchange with the outside world through respiration, evaporation, radiation, convection, and heat transfer can be regarded as the second and third types of boundary conditions, so the temperature distribution at the next moment can be calculated.

The temperature of the heart output port at the next moment is assigned to the blood vessel input to calculate the perfusion temperature. The skin temperature and hypothalamus temperature at this moment are assigned to the thermal regulation system, and the formula is substituted with the temperature at the previous moment and the set-point temperature to calculate the vasoconstriction and relaxation, as well as the sweating and vibration coefficient. And these coefficients are assigned to the blood perfusion rate of the heat source term in the unsteady heat conduction differential equation and the conditions of the heat production term and the surrounding boundary conditions of the human body, as well as the perspiration term in evaporation heat dissipation. In order to carry out the next calculation. Define $T_{(ijk)n+1} = T_{(ijk)0}$. The flow chart of the human thermal regulation model is shown in Fig. 3.
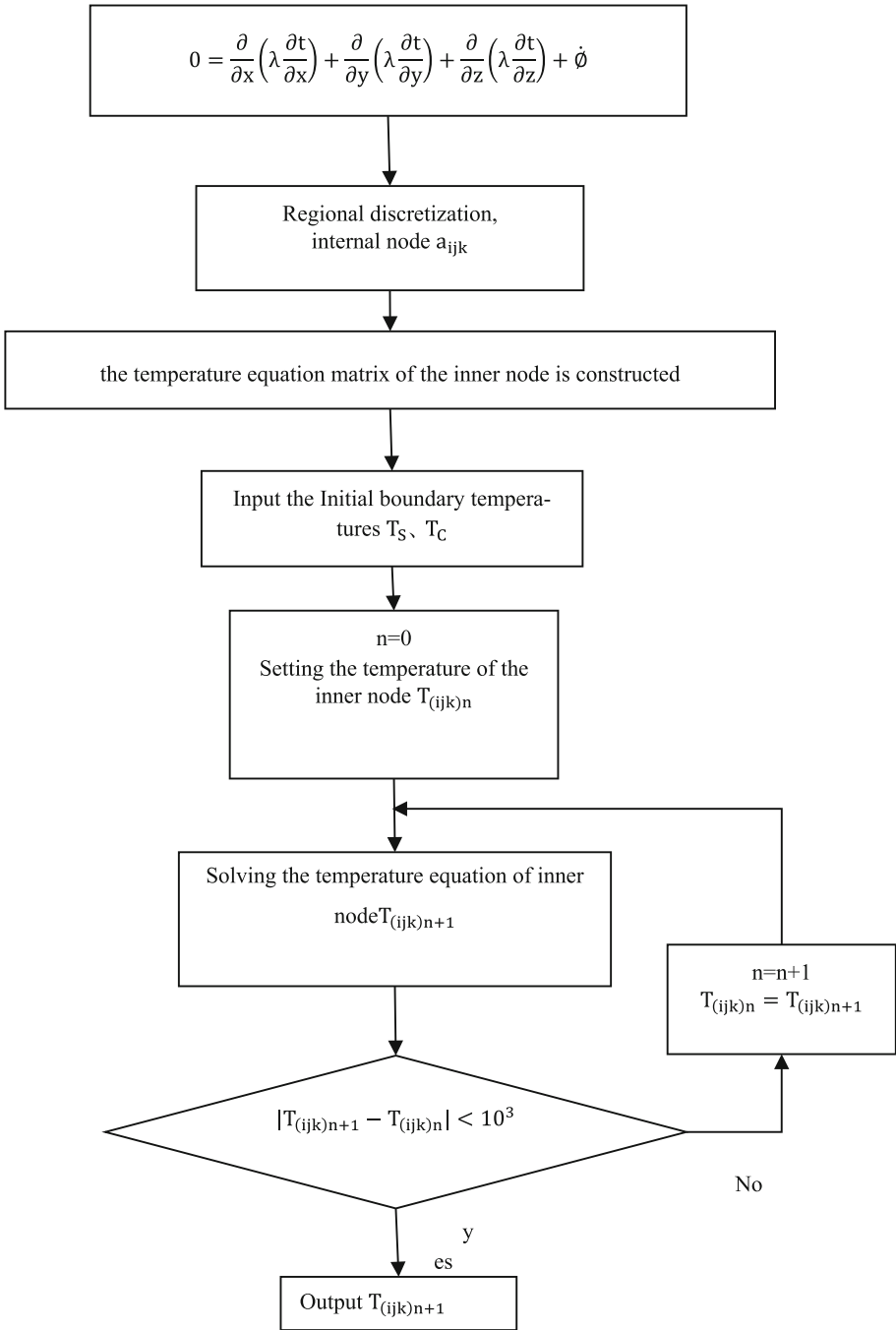
$$0 = \frac{\partial}{\partial x}\left(\lambda\frac{\partial t}{\partial x}\right) + \frac{\partial}{\partial y}\left(\lambda\frac{\partial t}{\partial y}\right) + \frac{\partial}{\partial z}\left(\lambda\frac{\partial t}{\partial z}\right) + \dot{\emptyset}$$

Regional discretization,
internal node $a_{ijk}$

the temperature equation matrix of the inner node is constructed

Input the Initial boundary tempera-
tures $T_S$、$T_C$

n=0
Setting the temperature of the
inner node $T_{(ijk)n}$

Solving the temperature equation of inner
node$T_{(ijk)n+1}$

n=n+1
$T_{(ijk)n} = T_{(ijk)n+1}$

$|T_{(ijk)n+1} - T_{(ijk)n}| < 10^3$

No

y
es

Output $T_{(ijk)n+1}$

**Fig. 2.** Initial temperature determination.
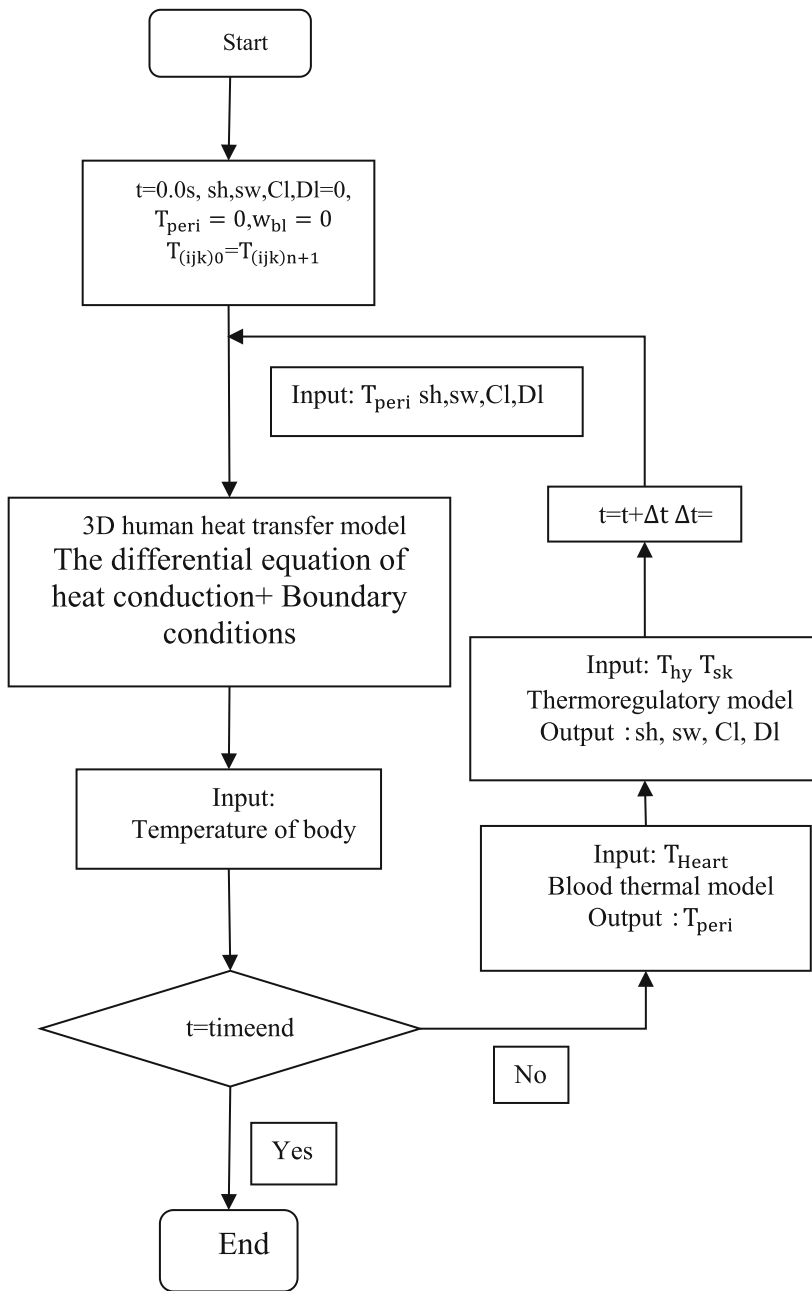
**Fig. 3.** Flow chart of the coupling thermal model.

# 3   Results and Discussion

## 3.1   The Conditions of Simulation

In this paper, the sitting posture model wearing shorts, T-shirt and sandals is used to simulate the human body temperature changes in hot and cold environments respectively. A human thermal regulation model is set up in the climate chamber. The size of the climate chambers was 3.5 m × 3.4 m × 2.0 m (length × width × height). The simulation is conducted in different environmental temperature. It's divided into cold, hot and comfortable environment. In this chapter, the simulation divided into the two parts.

First part:

The temperature of cold environment is about 20.1 °C, the temperature of hot environment is about 35.8 °C, and the neutral environment is about 29.2 °C. Using human skin temperature meter as initial temperature to input the model, then set the environment temperature 29.2 °C, and record the skin temperatures during 30 min, returned to the 20.1 °C during 20 min, back to the 29.2 °C for 30 min, and finally entered the 35.8 °C for 20 min [10]. The conditions are shown in Fig. 4.
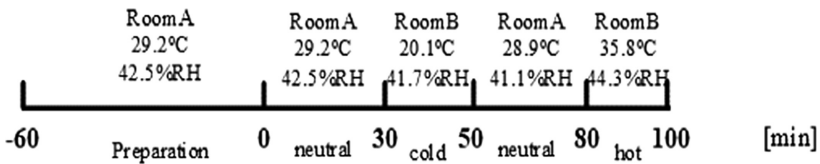


**Fig. 4.**  The condition of experiments.

Second part:

The human body wearing shorts at 29 °C and 40% humidity sits for half an hour, moves to 45 °C and 40% humidity, insists for half an hour, moves to 29 °C and 40% humidity for half an hour, and then enters 45 °C and 40% humidity for half an hour. The temperature data of skin nodes and rectal temperatures during these four time periods are recorded [11]. The human body wearing shorts at 29.4 °C and 46.6% humidity sits for 30 min, moves to 19.1 °C and 54.8% humidity, sits for 20 min, moves to 29.3 °C and 47% humidity and then insists for 40 min. The temperature data of skin nodes and rectal temperatures are recorded during these three time periods [12]. The conditions are shown in Table 2.

**Table 2.**  The condition of experiments.

|  |  | room-A | room-B | room-A | room-B |
|---|---|---|---|---|---|
| Hot weather | Time (min) | 30 | 30 | 30 | 30 |
|  | Air temperature °C | 29 | 45 | 29 | 45 |
|  | Globe temperature °C | 29 | 45 | 29 | 45 |
|  | Relative humidity (%) | 40 | 40 | 40 | 40 |
|  | Air velocity (m/s) | 0.06 | 0.06 | 0.06 | 0.06 |
|  | Time (min) | 30 | 20 | 40 |  |

(*continued*)

**Table 2.** (*continued*)

|  |  | room-A | room-B | room-A | room-B |
|---|---|---|---|---|---|
| Cold weather | Air temperature °C | 29.4 | 19.5 | 29.3 |  |
|  | Globe temperature °C | 29.5 | 20.4 | 29.4 |  |
|  | Relative humidity (%) | 46.8 | 52.8 | 47.1 |  |
|  | Air velocity (m/s) | 0.09 | 0.21 | 0.09 |  |

These two parts are different. The first part describes a continuous process of entering the cold environment first from neutral environment, into neutral environment and into thermal environment, while the second part describes respectively that neutral environment enters into thermal environment and finally into thermal environment and neutral environment enters into cold environment and enters neutral environment. The process of environment. Regardless of how the experiment is carried out, only different ambient temperature, humidity and wind speed are input into the simulation model. Therefore, the following parameters are input in the simulation, as shown in Table 3. The external temperature envelope of the human body is displayed in CFD as shown in Fig. 5.

**Table 3.** The simulate temperatures through CFD.

| Air temperature °C | 19.5 | 20.1 | 28.9 | 29 | 29.2 | 29.4 | 35.8 | 45 |
|---|---|---|---|---|---|---|---|---|
| Relative humidity % | 52.8 | 41.7 | 41.1 | 40 | 42.5 | 46.8 | 44.3 | 45 |
| Air velocity m/s | 0.21 | 0.06 | 0.05 | 0.06 | 0.01 | 0.09 | 0.07 | 0.06 |

The performance of the coupling system was examined by comparing the predicted skin temperatures with the measured ones from experiments. The RMSD values of skin temperatures at the segments of head, trunk, arm, hand, thigh, calf, and foot were 0.452 °C, 0.715 °C, 0.459 °C, 0.635 °C, 0.58 °C, 0.711 °C, and 0.645 °C respectively. The maximum difference between predicted temperatures and measurements at body segments was no more than 1.0 °C. The error analysis diagram of each temperature condition is shown in Fig. 6.

This chapter includes two parts. The first part The author compares the simulation model with the experiment done by the research group. The other part simulation model is compared with the experiment done by others in the references. By comparing the two parts, it can be seen that the experimental error of cold environment is not more than 0.771 °C and the hot environment is not more than 0.851 °C. The simulation system built by this paper can simulate the temperature changes of human body very well.
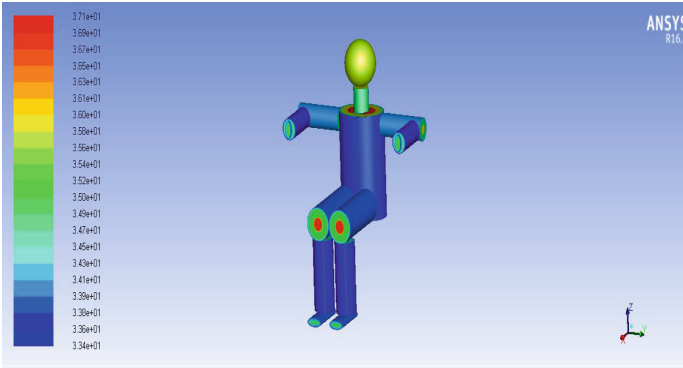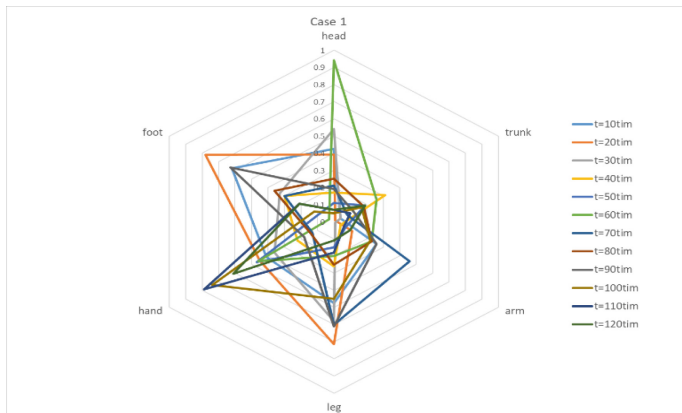
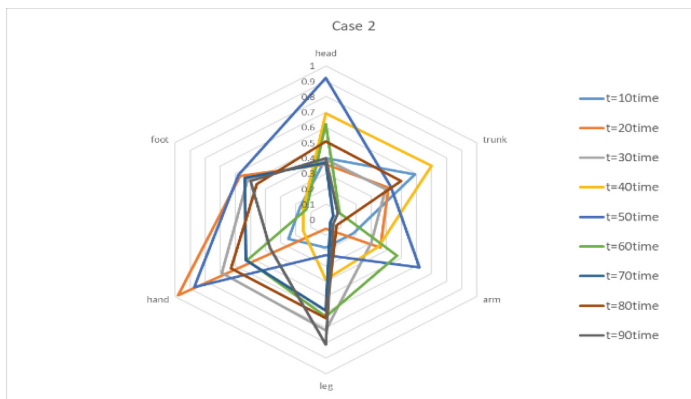(a)  Neutral environment
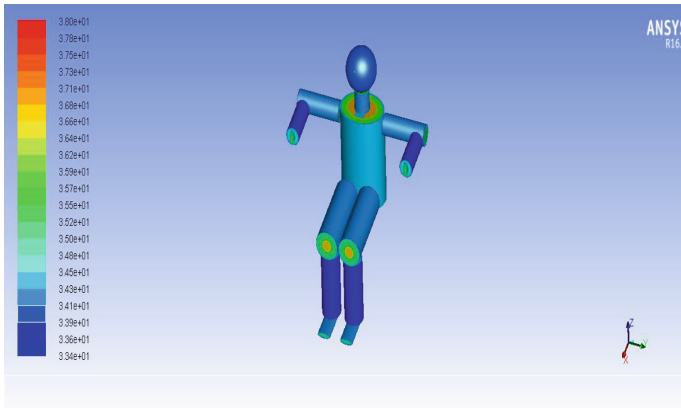


(b)  Cold environment
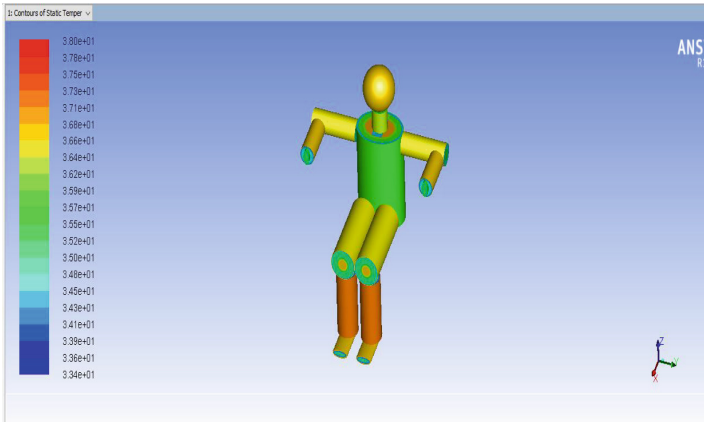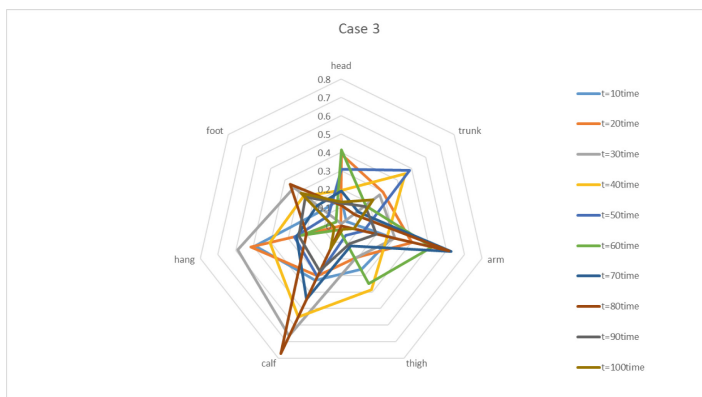


(c)  Hot environment

**Fig. 5.**  The conditions of simulation.

(a) Part 1 hot weather



(b) Part 2 cold weather



(c) Part 3 cold and hot weather

**Fig. 6.** Difference between the simulated skin temperatures by coupling system and those from human trials.

## 4   Conclusion

In this paper, CFD technology is used to simulate human thermal regulation system based on human pulsating flow and heat generation mechanism. The model is simulated in six parts. The first part simulates the structure of human body. The second part simulates the tissue heat transfer of human body. The third part simulates the perfusion temperature of blood in the heat source term. The fourth part simulates the boundary conditions. The fifth part simulates the regulation system. The sixth part is the coupling process between them. Finally, the visual simulation of the human body mathematical model is realized, which can simulate the thermal regulation of the human body very well. The accuracy of the simulation model are proved by comparing the results of other people's research with the experimental data of the research group.

However, whether the model established in this paper can be applied in the environment of instantaneous changes in the external environment is not yet validated. In the next work, the model parameters will be adjusted to adapt to the scene of instantaneous temperature change, and compared with the experimental results. The next work is to verify and revise the simulation model through unstable environmental experiments.

## References

1. Jiang, Y.Y., Yanai, E., Nishimura, K., et al.: An integrated numerical simulator for thermal performance assessments of firefighters' protective clothing. Fire Saf. J. **45**(5), 314–326 (2010)
2. Al-Othmani, M., Ghaddar, N., Ghali, K.: A multi-segmented human bioheat model for transient and asymmetric radiative environments. Int. J. Heat Mass Trans. **51**(23), 22–33 (2008)
3. Fiala, D., Lomas, K.J., Stohrer, M.: Computer prediction of human thermoregulatory and temperature responses to wide range of environmental conditions. Int. J. Biometeorol. **45**, 143–159 (2001)
4. Takada, S., Kobayashi, H., Matsushita, T.: Thermal model of human body fitted with individual characteristics of body temperature regulation. Built Environ. **44**(3), 46–70 (2009)
5. Zhang, Y., Yang, T.: Simulation of Human Thermal Responses in a Confined Space. ISIAQ, Copenhagen (2008)
6. Sina, D., Hongjun, X., Xiaoyan, Z., et al.: Three-dimensional human thermoregulation model based on pulsatile blood flow and heating mechanism. Chin. Phys. B **27**(11), 114402-1–114402-11 (2018)
7. Voigt, L.K.: NaviereStokes simulations of airflow in rooms and around a human body. Ph.D. thesis. Technical University of Denmark, Denmark (2001)
8. Tanabe, S., Kobayashi, K., Nakano, J., et al.: Evaluation of thermal comfort using combined multi-node thermoregulation (65MN) and radiation models and computational fluid dynamics (CFD). Energy Build. **34**, 637–646 (2002)
9. Yang, Y.: Indoor thermal response of human body in uniform environment (Warm Conditions). Ph.D. Thesis. Chongqing University (2015)
10. George, H., Dusan, F.: Thermal indices and thermophysiological modeling for heat stress. Compr. Physiol. **6**, 255–320 (2016)

11. Munir, A.: Re-evaluation of Stolwijk's 25-node human thermal model under thermal-transient conditions: prediction of skin temperature in low-activity conditions. Build. Environ. **44**, 1777–1787 (2009)
12. Yang, J., Weng, W., Zhang, B.: Experimental and numerical study of physiological responses in hot environments. J. Thermal Biol. **45**, 54–61 (2014)